PHYSICAL REVIEW B **77**, 081410(R) (2008)

# Numerical studies of conductivity and Fano factor in disordered graphene

C. H. Lewenkopf,[1,2] E. R. Mucciolo,[3] and A. H. Castro Neto[4]
[1]*Departamento de Física Teórica, Universidade do Estado do Rio de Janeiro, 20550-900 Rio de Janeiro, Brazil*
[2]*Harvard University, Department of Physics, Cambridge, Massachusetts 02138, USA*
[3]*Department of Physics, University of Central Florida, P.O. Box 162385, Orlando, Florida 32816, USA*
[4]*Department of Physics, Boston University, 590 Commonwealth Avenue, Boston, Massachusetts 02215, USA*
(Received 29 January 2008; published 27 February 2008)

Using the recursive Green's function method, we study the problem of electron transport in a disordered single-layer graphene sheet. The conductivity is of order $e^2/h$ and its dependence on the carrier density has a scaling form that is controlled solely by the disorder strength and the ratio between the sample size and the correlation length of the disorder potential. The shot noise Fano factor is shown to be nearly density independent for sufficiently strong disorder, with a narrow structure appearing at the neutrality point only for weakly disordered samples. Our results are in good agreement with experiments and provide a way for extracting microscopic information about the magnitude of extrinsic disorder in graphene.

DOI: 10.1103/PhysRevB.77.081410 PACS number(s): 73.23.−b, 73.50.−h, 81.05.Uw

Graphene, a two-dimensional (2D) allotrope of carbon with a honeycomb lattice, has attracted a lot of attention due to its unusual, Dirac-like, electronic spectrum, and its potential for an all-carbon based electronics.[1] While the theoretical literature on graphene is already quite extensive,[2] the effect of disorder on transport properties near the charge neutrality point (Dirac point) is still subject to much debate and controversy. The difficulty in understanding how disorder affects Dirac fermions has to do with the fact that electrochemical disorder is a relevant perturbation under the renormalization group and drives the system away from the weak disorder regime.[3] Hence, standard perturbation theory fails and one has to rely on either nonperturbative methods or numerical approaches. Although several recent theoretical works have been established that for short-range disorder large graphene samples should become insulators,[4] the current understanding of long-range disorder is less clear. Some authors[5] have questioned the existence of a beta function for undoped graphene while others[6] have proposed a nonmonotonic beta function for single-valley Dirac fermions and a metal-insulator transition. Numerical computations in momentum space[7] as well as simulations based on a transfer-matrix method[8,9] adapted to the single-valley Dirac equation[10] found instead a simple scaling law for the conductivity, a metallic beta function, and no indication of a new fixed point.[11] Furthermore, while the self-consistent Born approximation (SCBA) predicts a universal (impurity independent) conductivity of $4e^2/(\pi h)$,[12] percolation theory finds a smaller value.[13]

On the experimental side, graphene behaves as a good metal with conductivities of the order of $e^2/h$,[14] which is inconsistent with a purely ballistic transport. No sign of strong localization has been seen in graphene although the size of the samples (a few micrometers) may be smaller than the localization length in 2D.

Current experiments indicate that transport is not ballistic, but is it really diffusive? Experimentally, the electron mean free path $l_{\rm tr}$ can be estimated by gating graphene away from the Dirac point and using the Drude formula to relate $l_{\rm tr}$ to the conductivity $\sigma$: $l_{\rm tr}=\sigma/[(2e^2/h)\sqrt{\pi n}]$, where $n$ is the carrier density. Typically, $l_{\rm tr}$ is found to be smaller but close to the sheet linear size $L$. Although this estimate has to be taken with caution, it supports the notion that current experiments are in the crossover regime between ballistic and diffusive, a regime where standard analytical approaches fail. Establishing a quantitative understanding of the effect of disorder in the transport properties of graphene is of fundamental importance for the development of electronic devices where high mobilities are required. Therefore, an alternative theoretical study is desirable.

In this paper, we use the recursive Green's function method[15] to study numerically the effect of extrinsic long-range disorder in the linear electronic transport of graphene at low carrier densities. We explore the low-temperature limit, when intrinsic scattering mechanisms such as electron-phonon can be neglected. Our calculations are based on a microscopic, tight-binding model of the graphene sheet and performed at and near the Dirac point. After a simple rescaling, we find that the dependence of the conductivity on the carrier density is controlled only by a dimensionless disorder amplitude and the ratio of system size to disorder correlation length $L/\xi$. This dependence can vary from sublinear to superlinear, depending upon the disorder strength. Therefore, our results provide a way for extracting extrinsic disorder parameters from experimental data without making any assumption about the underlying dynamical regime. We also find that disorder has a marked effect on how the shot noise Fano factor depends on the carrier density. For samples with square aspect ratios and weak disorder, a narrow dip exists at the Dirac point, while for sufficiently strong disorder, the Fano factor becomes density independent, taking up values larger than $1/3$ that increase slowly with the disorder.

The nearest-neighbor tight-binding model on a honeycomb lattice with site disorder reads $H=-\Sigma_{\langle i,j\rangle}t|i\rangle\langle j| +\Sigma_i U(\mathbf{r}_i)|i\rangle\langle i|$, where $i$ and $\mathbf{r}_i$ label the lattice sites and their coordinates, respectively, and $t\approx 2.8$ eV is the hopping energy. The long-range disordered potential $U(\mathbf{r}_i)$ consists of $\mathcal{N}_{\rm imp}$ random lattice sites $\{\mathbf{R}_n\}$. Each of these sites is the center of a Gaussian scatterer with a random amplitude $U_n$ taken from a uniform distribution over the interval $[-\delta,\delta]$: $U(\mathbf{r}_i)=\Sigma_{n=1}^{\mathcal{N}_{\rm imp}}U_n e^{-|\mathbf{r}_i-\mathbf{R}_n|^2/2\xi^2}$, where $\xi>a_0$ is the range of the

 

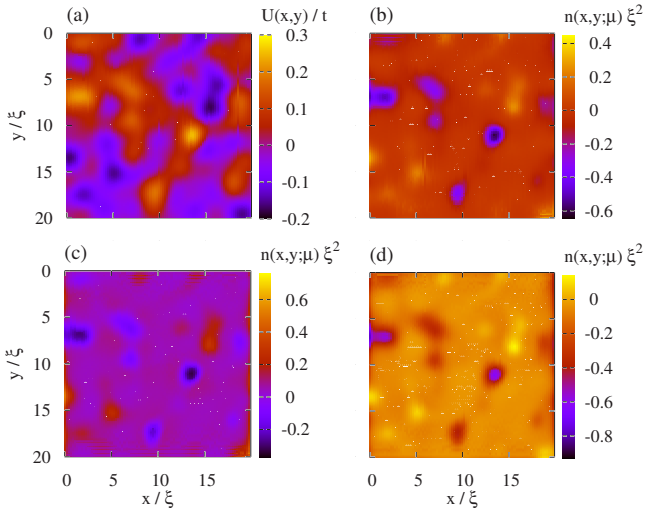


FIG. 1. (Color online) Color maps: (a) Long-range disordered potential in a square graphene sheet ($M=161$, $N=92$, $K_0=1$, $n_{\mathrm{imp}}=0.02$, $\xi=4a_0$). Carrier densities (positive for electron and negative for holes) at the Dirac point (b), above it (c), and below (d), with $\mu/t=0$, 0.1, and −0.1, respectively.

potential ($a_0\approx 2.46$ Å is the lattice constant).[16,17] A typical realization of the disorder is shown in Fig. 1(a). The concentration of scatterers is $n_{\mathrm{imp}}=\mathcal{N}_{\mathrm{imp}}/\mathcal{N}$, where $\mathcal{N}$ denotes the total number of atomic sites. When $n_{\mathrm{imp}}\ll 1$, the magnitude of the disorder fluctuations is characterized by the dimensionless parameter $K_0$, which is defined from the impurity potential correlation function

$$\langle U(\mathbf{r}_i)U(\mathbf{r}_j)\rangle = \frac{K_0(\hbar v)^2}{2\pi\xi^2} e^{-|\mathbf{r}_i-\mathbf{r}_j|^2/2\xi^2}, \qquad (1)$$

where $v=\sqrt{3}a_0t/2\hbar$ is the Fermi velocity [notice that $\langle U(\mathbf{r}_i)\rangle=0$]. We note that $K_0$ contains information not only about the relative magnitude of the potential fluctuations $\delta/t$ but also about the scatterers' range and concentration: A simple calculation yields $K_0\approx 40.5 n_{\mathrm{imp}}(\delta/t)^2(\xi/a_0)^4$.[17] In the continuum limit and using Eq. (1) together with the Born approximation (BA), one finds that the transport mean free path away from the Dirac point is given by $l_{\mathrm{tr}}^{\mathrm{BA}}=2\lambda_F/(\pi K_0)$, where $\lambda_F$ is the Fermi wavelength in the graphene sheet[16] ($\lambda_F\ll l_{\mathrm{tr}}^{\mathrm{BA}}$ for the BA to hold).

We investigate square graphene sheets with $M=1+2L/a_0$ and $N=1+2\sqrt{3}L/a_0$ lattice sites along perpendicular edges. The sheet is connected to ballistic, square lattice source, and drain leads following standard procedures.[15,18] For all data shown here, the edges parallel to the electron current flow are in the metallic armchair configuration[19] (we have found that, in the presence of disorder, similar results are obtained for the zigzag configuration). Using the recursive method, we compute the electron retarded Green's function at any lattice site $G^r(\mathbf{r}_i;E)$, where $E$ is the electron energy. The local density of states $\nu(\mathbf{r}_i;E)=-(1/\pi)\mathrm{Im}\,G(\mathbf{r}_i;E)$, is obtained and can be integrated in energy to yield the local carrier density at the Fermi energy $n(\mathbf{r}_i;\mu)=\int_{U(\mathbf{r}_i)}^{\mu}dE\,\nu(\mathbf{r}_i;E)$. This is illustrated in Figs. 1(b)–1(d), where we show the local carrier density for a fixed realization of the disorder potential and three values of the Fermi energy. The hole and electron puddles formed at the maxima and minima of the potential are clearly visible. These patterns are reminiscent of the single-electron transistor scannings of graphene.[20]

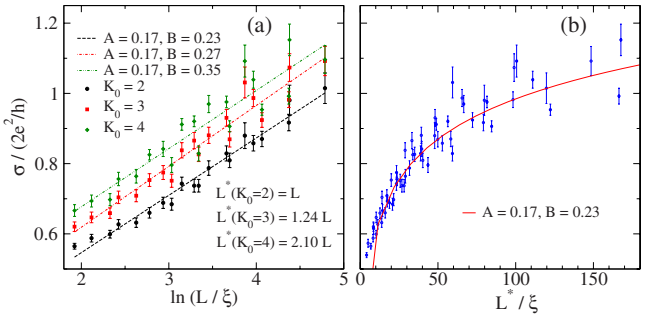


FIG. 2. (Color online) (a) Scaling of the average conductivity with sample size for a square graphene sheet at the Dirac point. The data corresponds to $M=41,83,113,161,317,479$, $\xi/a_0=2,3,5$, and $n_{\mathrm{imp}}=0.02$. The lines denotes the best-fits of the form $\sigma/(2e^2/h)=A\ln(L/\xi)+B$ to the data. (b) Average conductivity versus rescaled sheet lengths $L^*=\alpha(K_0)L$, with $\alpha$ determined from the best-fits found in (a).

The recursive Green's function method provides an efficient way to compute the electron's scattering matrix as a function of the electron energy $S(E)$. From $S$, one obtains the transmission $t$ and reflection $r$ matrices, which are then used in the computation of the linear conductance $\mathcal{G}$ and the shot noise Fano factor $F$: $\mathcal{G}=(2e^2/h)\mathrm{Tr}(tt^\dagger)$ and $F=\mathrm{Tr}(t^\dagger tr^\dagger r)/\mathrm{Tr}(t^\dagger t)$ (the factor of 2 in $\mathcal{G}$ accounts for spin degeneracy). We note that $\sigma=\mathcal{G}$ for a square sheet.

In Fig. 2, we show the scaling of the conductivity with $L$ at the Dirac point for several disorder strengths and correlation lengths. Our results are in qualitative agreement with recent numerical studies using the continuum model[7–9] and are compatible with a metallic beta function of the form $\beta(\sigma)=A(2e^2/h)/\sigma$, with $A\approx 0.17$. In particular, the quantitative agreement with the scaling obtained in Refs. 7 and 8 indicates that for correlation lengths $\xi\gtrsim 2a_0$, there is no noticeable effect of intervalley scattering. Thus, the lattices in our study are large enough to reproduce the numerical results obtained with the continuous single-valley model.

In order to explore how the conductivity behaves as a function of carrier density $n$, we compute the latter as a function of the Fermi energy $\mu$ in the graphene sheet through the expression $n(\mu)=\int_0^{\mu}dE\,\nu(E)$, where $\nu(E)$ is the sheet global density of states (DOS), which can be readily obtained from the energy dependence of the scattering matrix. By writing the scattering matrix in terms of the retarded Green's functions,[15] one can show that the Wigner-Smith time delay $\tau_W(E)=-i\hbar(d/dE)\ln(\det S)$, becomes $\tau_W(E)=-2\hbar\,\mathrm{Tr}[\mathrm{Im}\,G^r(\mathbf{r}_i;E)]$. We thus arrive at $\nu(E)=-(i/\pi WL)\mathrm{Tr}[S^\dagger(dS/dE)]$. These steps show that $\nu=2\tau_W/(hWL)$, as expected from scattering theory.

In Fig. 3(a), we show the average $\nu(E)$ for different values of the disorder parameter $K_0$ and a fixed $\xi$. Notice that the DOS does not vanish at the Dirac point, as one expects for an

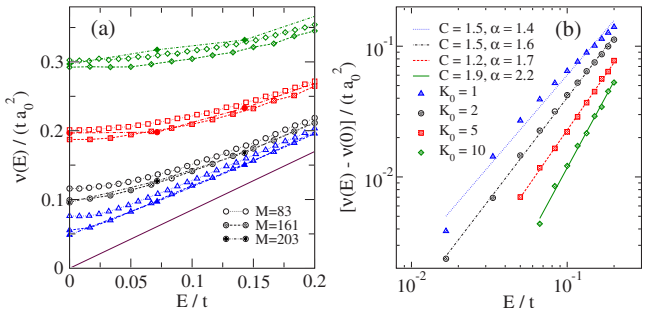


FIG. 3. (Color online) (a) Average density of states for three lattice sizes (different symbols) and four values of $K_0$ (different colors and line types). Notice that $L=(M-1)a_0/2$. Only data for $E>0$ is shown. The thick solid line represents the case of a clean, infinite graphene sheet, and the other lines are guides to the eyes. The number of realizations varies from 100 to 10 000 with $\xi=2a_0$ and $n_{\mathrm{imp}}=0.02$. (b) Shifted density of states for $M=161$. The lines correspond to best fits of the form $\nu(E)-\nu(0)=Cta_0^2|E/t|^{\alpha}$.

infinite clean graphene sheet. The coupling to the semi-infinite leads broadens the electronic energy levels in the graphene sheet, an effect that is more pronounced in the vicinity of the Dirac point. More interesting, however, is the effect of disorder. We observe that as $K_0$ increases, the DOS becomes almost flat over a large energy range. In particular, close to the Dirac point the DOS grows substantially with $K_0$, surpassing the broadening due to the coupling to the leads.

Remarkably, we find numerical evidence that the DOS is very robust against system size scaling. Figure 3(a) shows that $\nu(E)$ rapidly converges as $M$ is increased and $K_0<10$. Another feature worth noticing is that, for strong enough disorder, $\nu(E)$ grows approximately as a power law with $E$, as shown in Fig. 3(b). Our results for the DOS complement the analysis of Ref. 3 of the problem of Dirac fermions in the presence of a random chemical potential. This kind of disorder was shown to be a relevant perturbation in the renormalization group sense, possibly taking the system to a new fixed point if electron-electron interactions are taken into account.[6]

We now turn our attention to transport properties. Our main results are collected in Fig. 4. As one departs from the Dirac point, the counterintuitive feature that the conductivity is enhanced by disorder disappears.[10] For a fixed disorder, the conductivity increases with carrier density. By plotting $\sigma$ as a function of the number of electrons contained in a square of area $\xi^2$, we find that the functional dependence is solely controlled by the disorder strength $K_0$ and the ratio $L/\xi$. Notice that $\sigma$ as a function of $n\xi^2$ goes from sublinear (weak disorder) to linear (intermediate disorder) and then to superlinear (strong disorder) as $K_0$ is varied. All three behaviors are seen in the experiments[14] and therefore may be related to the strength of the long-range disorder in the samples. For a fixed $K_0$ and dilute scatterers, we found little dependence of our results on $n_{\mathrm{imp}}$.

The scaling behavior of $\sigma=\sigma(n\xi^2,K_0,L/\xi)$ works in the crossover regime from ballistic to diffusive regimes and departs strongly from the SCBA prediction,[16] which is only justifiable in the semiclassical diffusive regime, when $\lambda_F \ll l_{\mathrm{tr}}^{\mathrm{BA}} \ll L$. Notice that $l_{\mathrm{tr}} \lesssim \lambda_F$ in Fig. 4 and therefore our simulations are far from the semiclassical limit. Although the lattices investigated are rather small in comparison to the graphene samples probed in experiments, the scaling allows us to make a direct comparison with experimental data by using realistic values of $\xi$ (which ranges between 10 and 100 nm, as shown in Ref. 20) and extrapolating the $\sigma$ curves to large carrier densities, typically of order $10^{12}$ cm$^{-2}$. This in turn provides a way for estimating the value of $K_0$ in transport measurements dominated by extrinsic disorder. As an example, in Fig. 4, if we take $L/\xi=20$ and $K_0=2$ [which yields an approximately linear $\sigma(n)$ dependence] and assume $\xi=50$ nm, we obtain $\sigma\approx 500e^2/h$ for densities of order $10^{12}$ cm$^{-2}$, which is just a bit higher than the value measured experimentally in high mobility samples.

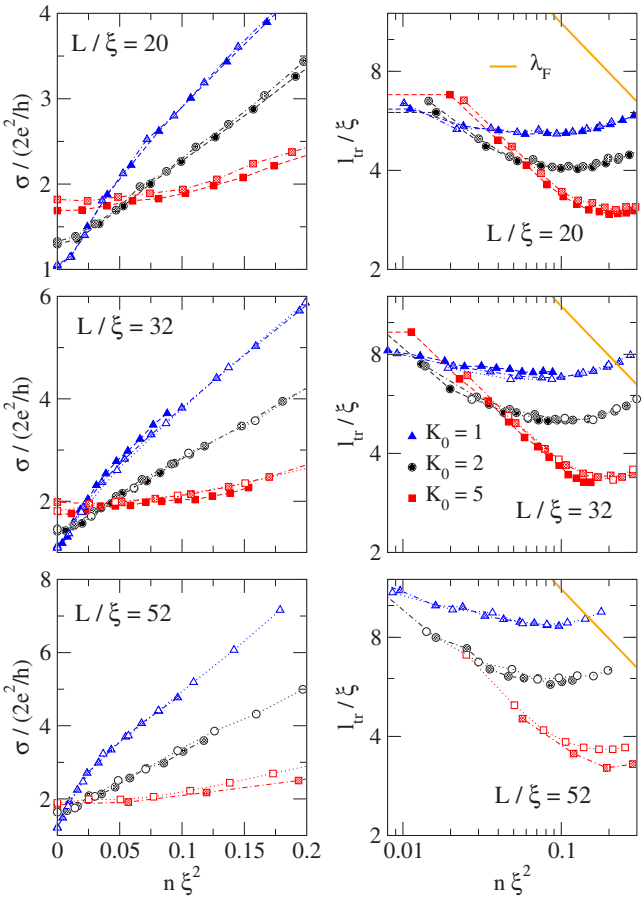


FIG. 4. (Color online) Average conductance (left column) and Drude transport mean free path (right column) as functions of carrier density for several disorder strengths ($K_0=1,2,5$), lattice sizes ($L/a_0=80,101,164$), and disorder correlation lengths ($\xi/a_0=2,2.5,3,3.3,4,5$). The number of realizations varies from 100 to 5000 depending on $K_0$ and $L$. The thick solid line corresponds to the clean system Fermi wavelength $\lambda_F=2\sqrt{\pi/n}$. The transport mean free path is calculated using $l_{\mathrm{tr}}=\sigma/[(2e^2/h)\sqrt{\pi n}]$.

In Fig. 5, we present the typical dependence of the average Fano factor on the carrier density and disorder strength for square and rectangular sheets. For weakly disordered square samples, we observe a narrow dip at the Dirac point followed by a saturation of $F$ as $n$ is increased. As the disorder increases, the dip rapidly disappears and $F$ takes a

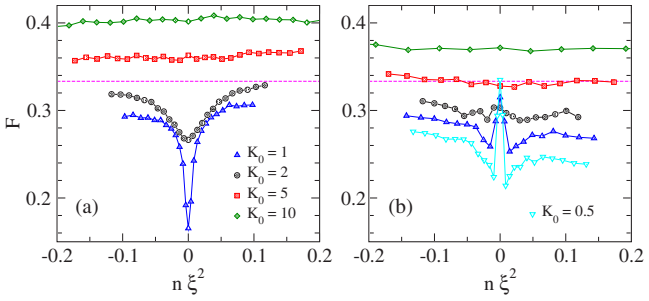


FIG. 5. (Color online) Average Fano factor as a function of carrier density for several disorder strengths and $\xi=2a_0$. The number of realizations ranges from 100 to 5000. (a) Square sheets ($W/L=1$) with $L/\xi=40$. (b) Rectangular sheets ($W/L=3.1$) with $L/\xi=26$. The dashed lines represent $F=1/3$.

density-independent value above $1/3$, which is the value expected for a normal metal in the diffusive regime.[22] In contrast to the behavior seen for the conductivity, we do not observe a clear scaling behavior for $F$, namely, the data do not collapse onto distinct universal curves when sorted out by $K_0$ and $L/\xi$ (not shown). For short and wide rectangular sheets, the behavior is quite distinct from the square case. For weak disorder, there is a peak located at the Dirac point, followed by a damped oscillation towards a saturation value (the asymmetry is due to a band mismatch between the honeycomb and lead lattices). These features are compatible with analytical results derived for clean junctions with large $W/L$ aspect ratios.[21] As the disorder strength increases, the peak widens, the oscillations are smeared, and the saturation value of $F$ goes up. For large disorder strengths, $F$ becomes again nearly density independent. For both geometries, the behavior we obtain for strong disorder appears consistent with recent experiments by DiCarlo *et al.*, who found a nearly density-independent $F$ for several graphene samples.[23] However, this behavior departs from the results of other numerical simulations, where a saturation value near 0.3 was found.[9] Notice that the dip (square samples) and the peak (rectangular samples) near the Dirac point disappear rapidly as the disorder strength is increased and therefore can be interpreted as indicative of very weak disorder. Danneau *et al.* have recently reported the observation of ballistic behavior in their measurements of the Fano factor for samples where $W/L \gg 1$,[24] although the width of the peak in their experiment is nearly two orders of magnitude larger than the theoretical prediction for clean samples.[21]

In summary, we have performed numerical simulations to evaluate the conductivity and the shot noise Fano factor in graphene samples as a function of carrier density and in the presence of long-range disorder. We found that the conductivity follows universal scaling curves that depend solely on the disorder strength and the ratio of sheet length to disorder correlation length. The Fano factor was found to have a marked dependence on the density only for very weak disorder and near the Dirac point. For moderate to strong disorder, the Fano factor is nearly constant and its value is not universal. While our model of long-range disorder applies mainly to situations where the strong modulation of the potential in the graphene sheet is due to roughness in the substrate, it could also be extended to account for the effect of charge impurities present in the substrate or on the graphene sheet. The only necessary modification is the inclusion of a density-dependent correlation length $\xi$ to take into account screening by carriers in the graphene sheet. However, this modulation of $\xi$ should be weak for the low densities we have been able to study.

We thank H. Baranger, L. DiCarlo, A. Geim, F. Guinea, P. Kim, C. Marcus, A. Mirlin, J. R. Williams, and A. Yacoby for illuminating discussions. C.H.L. thanks CAPES (Brazil) and the Institute of Quantum Science and Engineering at Harvard for support.

[1] A. K. Geim and K. S. Novoselov, Nat. Mater. **6**, 183 (2007).
[2] A. H. Castro Neto *et al.*, arXiv:0709.1163 (unpublished).
[3] A. W. W. Ludwig, M. P. A. Fisher, R. Shankar, and G. Grinstein, Phys. Rev. B **50**, 7526 (1994).
[4] A. Altland, Phys. Rev. Lett. **97**, 236802 (2006).
[5] K. Nomura and A. H. MacDonald, Phys. Rev. Lett. **98**, 076602 (2007).
[6] P. M. Ostrovsky, I. V. Gornyi, and A. D. Mirlin, Phys. Rev. Lett. **98**, 256801 (2007).
[7] K. Nomura, M. Koshino, and S. Ryu, Phys. Rev. Lett. **99**, 146806 (2007).
[8] J. H. Bardarson, J. Tworzydlo, P. W. Brouwer, and C. W. S. Beenakker, Phys. Rev. Lett. **99**, 106801 (2007).
[9] P. San-Jose, E. Prada, and D. S. Golubev, Phys. Rev. B **76**, 195445 (2007); E. Louis, J. A. Vergés, F. Guinea, and G. Chiappe, *ibid.* **75**, 085440 (2007).
[10] M. Titov, Europhys. Lett. **79**, 17004 (2007).
[11] S. Ryu, C. Mudry, H. Obuse, and A. Furnsaki, Phys. Rev. Lett. **99**, 116601 (2007).
[12] E. Fradkin, Phys. Rev. B **33**, 3257 (1986).
[13] V. V. Cheianov *et al.*, Phys. Rev. Lett. **99**, 176801 (2007).
[14] S. Cho and M. S. Fuhrer, Phys. Rev. B **77**, 081402(R) (2008); Y.-W. Tan *et al.*, Phys. Rev. Lett. **99**, 246803 (2007); J. G. Checkelsky, L. Li, and N. P. Ong, arXiv:0708.1959 (unpublished); S. V. Morozov *et al.*, Phys. Rev. Lett. **100**, 016602 (2008).
[15] P. A. Lee and D. S. Fisher, Phys. Rev. Lett. **47**, 882 (1981).
[16] N. H. Shon and T. Ando, J. Phys. Soc. Jpn. **67**, 2421 (1998); P. M. Ostrovsky, I. V. Gornyi, and A. D. Mirlin, Phys. Rev. B **74**, 235443 (2006).
[17] A. Rycerz, J. Tworzydło, and C. W. J. Beenakker, Europhys. Lett. **79**, 57003 (2007).
[18] H. Schomerus, Phys. Rev. B **76**, 045433 (2007).
[19] L. Brey and H. A. Fertig, Phys. Rev. B **73**, 235411 (2006).
[20] J. Martin *et al.*, Nat. Phys. **4**, 144 (2008); M. Ishigami *et al.*, Nat. Mater. **7**, 1643 (2007).
[21] J. Tworzydło, B. Tranzettel, M. Titov, A. Rycerz, and C. W. J. Beenakker, Phys. Rev. Lett. **96**, 246802 (2006).
[22] Ya. M. Blanter and M. Büttiker, Phys. Rep. **336**, 1 (2000).
[23] L. DiCarlo *et al.*, arXiv:0711.3206 (unpublished).
[24] R. Danneau *et al.*, arXiv:0711.4306 (unpublished).